TECHNICAL NOTE: CT CALIBRATION FOR PROTON TREATMENT PLANNING BY CROSS-CALIBRATION WITH PROTON CT DATA

ABSTRACT

Purpose: This study explores the possibility of a new method for x-ray computed tomography (CT) calibration by means of cross-calibration with proton CT (pCT) data. The proposed method aims at a more accurate conversion of CT Hounsfield Units (HU) into proton stopping power relative to water (SPR) to be used in proton-therapy treatment planning.

Methods: X-ray CT scans were acquired on an anthropomorphic phantom, composed of different tissue equivalent materials (TEMs). A pCT apparatus was instead adopted to obtain a reference 3D distribution of the phantom's SPR values. After rigid registration, the x-ray CT was artificially blurred to the same resolution of pCT. Then a scatter plot showing voxel-by-voxel SPR values as a function of HU was employed to link the two measurements and thus obtaining a cross-calibrated x-ray CT calibration curve. The cross-calibration was tested at treatment planning system and then compared with a conventional calibration based on exactly the same TEMs constituting the anthropomorphic phantom.

Results: Cross-calibration provided an accurate SPR mapping, better than by conventional calibration. The dose distribution of single beams optimized on the reference SPR map was compared with the recalculations computed on cross-calibrated CT, showing minor deviation at the dose fall-off, with range uncertainty lower than 1%.

Conclusions: The presented data demonstrated that, by means of reference pCT data, a heterogeneous phantom can be used for CT calibration, paving the way to the use of biological samples, with their accurate description of patients' tissues. This overcomes the limitations of conventional CT calibration requiring uniform samples, which can be only obtained by synthetic TEMs, which fails in accurately mimicking the properties of biological tissues. Once a heterogeneous biological sample is provided with its corresponding SPR maps, a cross-calibration procedure could be adopted by other PT centers, even when not equipped with a pCT system.

Keywords: CT; proton CT; proton therapy

INTRODUCTION

In proton therapy (PT), the dose computation is based on x-ray computed tomography (CT) images of the patient, which are acquired to account for the effect of tissue inhomogeneity. The CT Hounsfield Units (HU) are converted by a CT calibration into proton stopping power ratio (SPR), relative to water. The proton SPR is then used for dose computation in the treatment planning systems. Uncertainties in proton range can have a profound effect on proton treatments and one of the main sources of uncertainty is currently represented by inaccuracies in the CT calibration.[1] Since range uncertainty is still an unresolved issue in PT it is a common practice to assume an uncertainty of about 3% in the estimated particle range, compensating for that in the planning phase and thus leading to an increased volume of healthy tissue being irradiated. In principle, by decreasing the uncertainty on the proton estimated range with an improved CT calibration method, it would be possible to significantly reduce the irradiated healthy tissues surrounding the tumour, thus obtaining an increased treatment conformity.

For these reasons, different methods for x-ray CT calibration are under continuous investigation.[2,3,4] Conventionally, single-energy CT calibration is obtained by scanning a number of tissue equivalent materials (TEMs), which have limitations in mimicking the properties of real tissues. To partially overcome that issue, a stoichiometric calibration has been proposed or, more recently, dual-energy CT methods were investigated.[2,3,5] In general, in these methods the CT calibration is a procedure performed in two steps.[6] The first step involves the computation of the relative electron or mass density and in some cases of the effective atomic number. The second step consists in the translation of such quantities into proton SPR by an heuristic function, which depends on specific material related properties such as the mean excitation energy. In principle, accurate SPR maps could be directly obtained by proton computed tomography (pCT), thus overcoming any limitation in the accuracy of such two-steps procedures. Unfortunately, clinically approved pCT systems are not yet available to be routinely used on patients.

Direct methods for CT calibrations were proposed in a few studies. Those methods are based on the use of additional water equivalent thickness (WET) measurements to determine a relationship between CT numbers and SPR. Schneider et al[7] anticipated this intriguing concept in an experimental model, by optimizing x-ray CT calibration using in-vivo proton radiography. This method operates in the projection-domain, being based on the use of projected images (proton radiographies, 2D) to optimize the HU-SPR conversion. In successive studies, the combination of x-ray CT with WET data was investigated in different scenarios. CT was optimized by i) one-dimensional data obtained by range probing on biological phantoms,[8] ii) in the projection-domain, two-dimensional data obtained by proton radiography (theoretically[9,10,11] and experimentally[8]

investigated) and finally, iii) multiple two-dimensional data obtained by multiple projection proton radiography on a tissue equivalent phantom.[12] In this context it is reasonable to expect that increasing the quantity of additional WET data, from 1D to multiple 2D, may allow an improved and more robust solution to obtain an optimized x-ray CT calibration curve and that the best performances could be obtained by full 3D data, i.e. by pCT. Methods that work with the pixel values in 3D pCT reconstructed images can be considered as image-domain methods. So far, the most advanced dual-energy CT methods were compared with pCT,[13] but pCT has never been used to optimize x-ray CT calibration.

In the present preliminary study, we aim to investigate the possibility of x-ray CT calibration by cross-calibration with pCT data, presenting and discussing a first image-domain methodological approach on a synthetic anthropomorphic phantom. Even though pCT is not yet clinically available, it has been experimentally developed and it could be used to scan suitable biologic phantom to be used to cross calibrate x-ray CT for PT treatment planning.

MATERIALS AND METHODS

Proton and x-ray CTs were acquired on a neck portion of the head anthropomorphic phantom Model 731-HN (CIRS, Inc., Norfolk, VA, USA), composed of different TEMs. Small uniform cylinders (length 50mm, ∅ 30 mm) were also available for the TEMs, separately from the head phantom.

A detailed description of our pCT apparatus with tomographic reconstructions is reported elsewhere.[14] In summary, the pCT system is made of four planes of silicon microstrip tracker and a YAG:Ce scintillating calorimeter. The object to be imaged is placed on a remotely controlled rotating platform, between the second and third tracker plane, while the calorimeter is positioned just after the fourth plane. For each proton, the tracker reconstructs the two trajectory segments upstream and downstream of the phantom, while the calorimeter measures the residual energy. A number of protons of the order of 10^8 while rotating the phantom in 400-800 angle positions were acquired. Thus an algebraic iterative algorithm was applied to reconstruct SPR 3D distribution, with voxel size 0.6x0.6x0.8 mm^3.

Conventional x-ray CT scans were acquired at single energy (120 kV) in a 512×512 matrix with voxel size 0.8x0.8x1.0 mm^3 by a big bore Brilliance CT scanner (Philips Medical Systems, Cleveland, OH, USA).

Cross calibration was obtained after pCT and x-ray CT data alignment by rigid registration, which is legitimate when using non-moving phantoms. Image processing was performed by MATLAB® (The MathWorks.inc, Natick, MA, USA). After rigid alignment of the data by an intensity-based method, a volume of interest was selected considering all the voxel with SPR>0.5 in the pCT images. In order to account for the different image quality of the two modalities, the x-ray CT was artificially blurred with an averaging filter to degrade the spatial resolution to a level comparable to the lower resolution of pCT. A scatter plot was then obtained showing the voxel-by-voxel SPR versus HU values, which were used to extract the calibration curve. In details, the data points belonging to the volume of interest were sorted according to increasing HU and grouped in equal-sized bins. For each bin, the mean values of the SPR was calculated and plotted against the corresponding mean HU values. The CT calibration curve is thus obtained by the line connecting the resulting mean data points. The effect of different bin sizes was preliminarily assessed, considering that a small bin size corresponds to few data points and a resulting noisy lookup table, while too large bins might smooth significant variations in the HU-SPR relationship.

Differential maps were computed to perform a consistency test of the procedure. In details, the calibration curve obtained by cross-calibration was used to compute the synthetic SPR map, which was compared with the reference SPR map measured by pCT by means of a differential map.

A difference map was also computed between the synthetic SPR map obtained by conventional x-ray CT calibration (see details below) minus the reference SPR map measured by pCT.

The cross calibration procedure was verified on a commercial (RaySearch Laboratories, Stockholm, Sweden) treatment planning system (TPS). At TPS, the delivery of uniform dose by a single proton beam optimization (SFO) to an exemplary target was simulated. SFO is best suited to visualize range difference as there is a single distal surface of the dose volume and distal energy layers have the highest weight. On the other hand, it is worth mentioning that multi field optimisation has become clinical routine[15] and the effect of range uncertainties can be slightly different in that case. The optimization was run on the SPR map obtained from pCT images. The dose delivered by the obtained spot distribution was then recalculated using the SPR map derived from X-ray CT images by i) CT cross-calibration and ii) conventional x-ray CT calibration. The latter was obtained exploiting the uniform cylinders made of the same TEMs as the head phantom. For this purpose, the cylinders were inserted in the corresponding holes of a plastic water phantom (180 mm diameter, 50 mm length) and scanned with the same x-ray CT acquisition protocol used for the head phantom. A small region of interest was drawn on each cylinder and the corresponding mean HU values were calculated. Starting from the mass density of the TEMs and the corresponding mean HU, a standard CT calibration curve was obtained at the TPS. The conversion of mass density into SPR is then performed by the TPS, by means of a dedicated algorithm checking on a list of about fifty fixed materials,[16] created by interpolation from a number of well-established core materials. Each CT voxel is thus associated with the material closest in mass density and its atomical composition as well as the mass density associated to the voxel is used to compute the SPR.

RESULTS

A section of the head anthropomorphic phantom is shown in **Figure 1A**, where the different TEMs are visible in different colours (soft tissue in grey, spinal cord in yellow and trabecular bone in brown). For these three types of TEMs a corresponding uniform rod cylinder was available (**Figure 1B**), which was used for validation measurements. In the head phantom section there are other visible TEMs, such as vertebral disk (in white) and a thin cortical layer (in grey). However, for these tissue types a rod TEMs was not available to perform a corresponding validation.

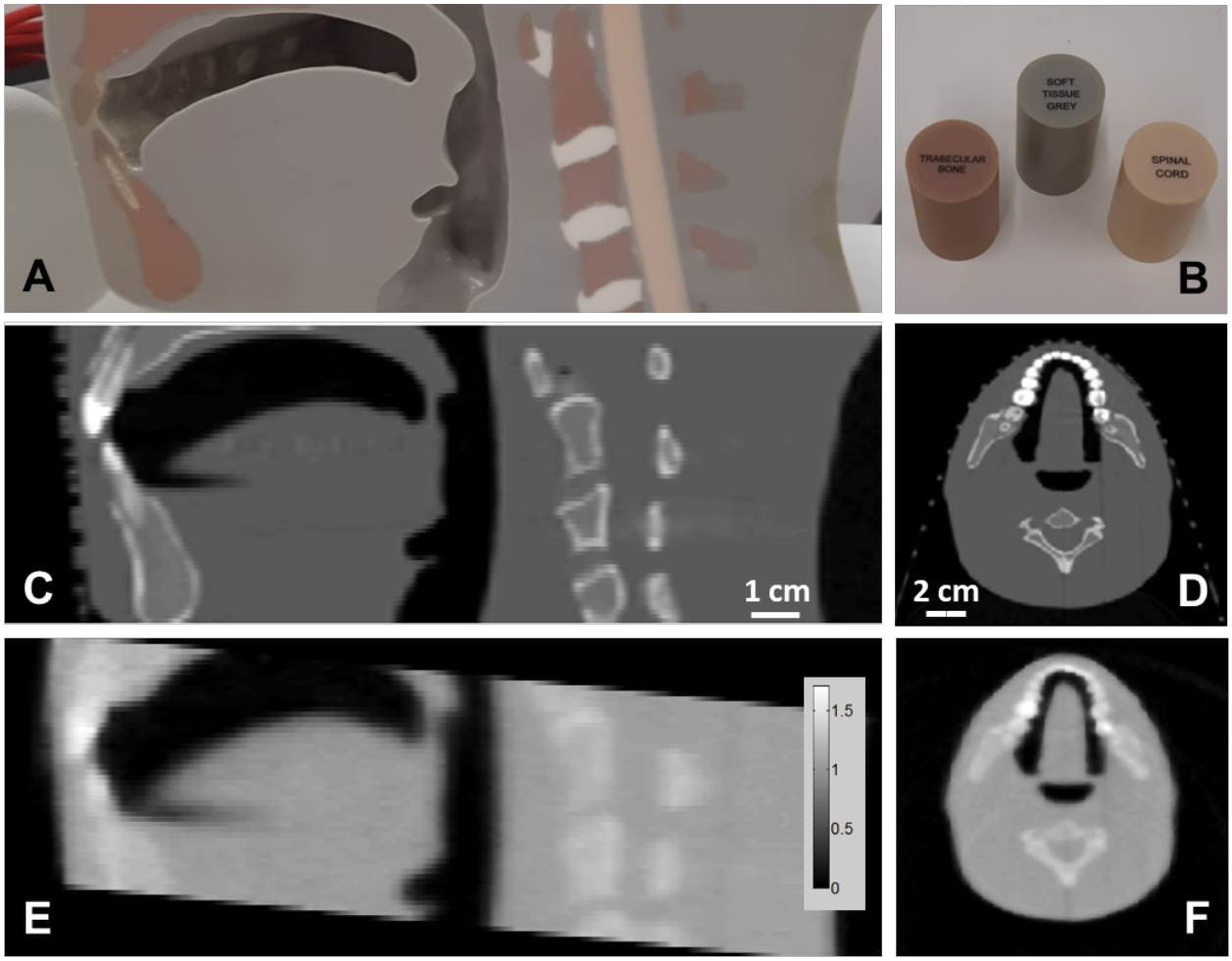

Figure 1. A section of the head anthropomorphic phantom Model 731-HN (**A**), made of different tissue equivalent materials (TEMs). Small uniform cylinders available for three of the TEMs (**B**), i.e. soft tissue (1.05 g/cm3), spinal cord (1.07 g/cm3) and trabecular bone (1.16 g/cm3). X-ray CT sagittal (**C**) and axial (**D**) projections. Proton CT sagittal (**E**) and axial (**F**) projections. In (**E**) the greyscale represent SPR values.

The x-ray CT images (**Figure 1C-D**) were registered with pCT images (**Figure 1E-F**), thus obtaining a voxel-by voxel correspondence between HU and SPR, as reported in a scatter plot (**Figure 2A**).

The effect of different bin size to obtain the calibration curve was preliminarily assessed at 10, 50 and 100 HU (**Figure3**), confirming that increasing bin size may produce undesired

smoothing, while reducing bin size introduces noise in the calibration curve. According to the reported data, a bin size collecting around 500 voxels (i.e. around 0.3 cm^3), with bins spaced every 50 HU seems to produce an acceptable curve. That volume could be reduced by decreasing the noise in the source data, e.g. by increasing the CTs acquisition time. The calibration curve obtained by 50 HU bin size is also shown in **Figure 2A** and it has been used in the following.

Differential maps of the synthetic SPR map minus the measured pCT were computed to perform a consistency test of the procedure and are reported in **Figure 2B-C**. They evidenced a better agreement by the calibration obtained by cross-calibration with respect to that obtained by conventional x-ray CT calibration.

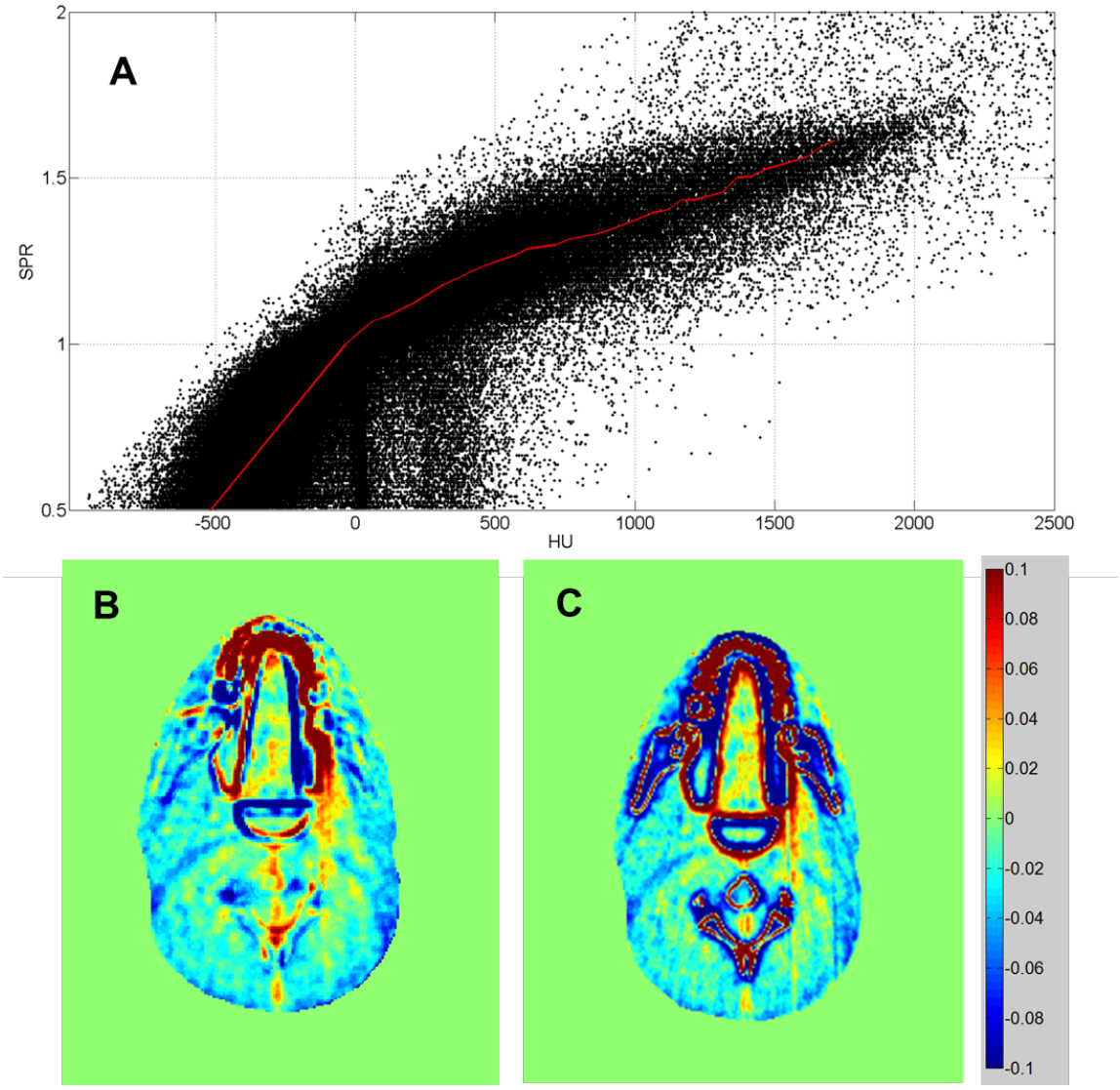

Figure 2. Proton CT SPR vs HU x-ray scatter plot (**A**). The calibration curve obtained by cross-calibration is shown as a red line. Difference between the SPR map obtained by cross-calibration minus the SPR map obtained by pCT (**B**). Difference between the SPR map obtained by conventional x-ray CT calibration minus the SPR map obtained by pCT (**C**).

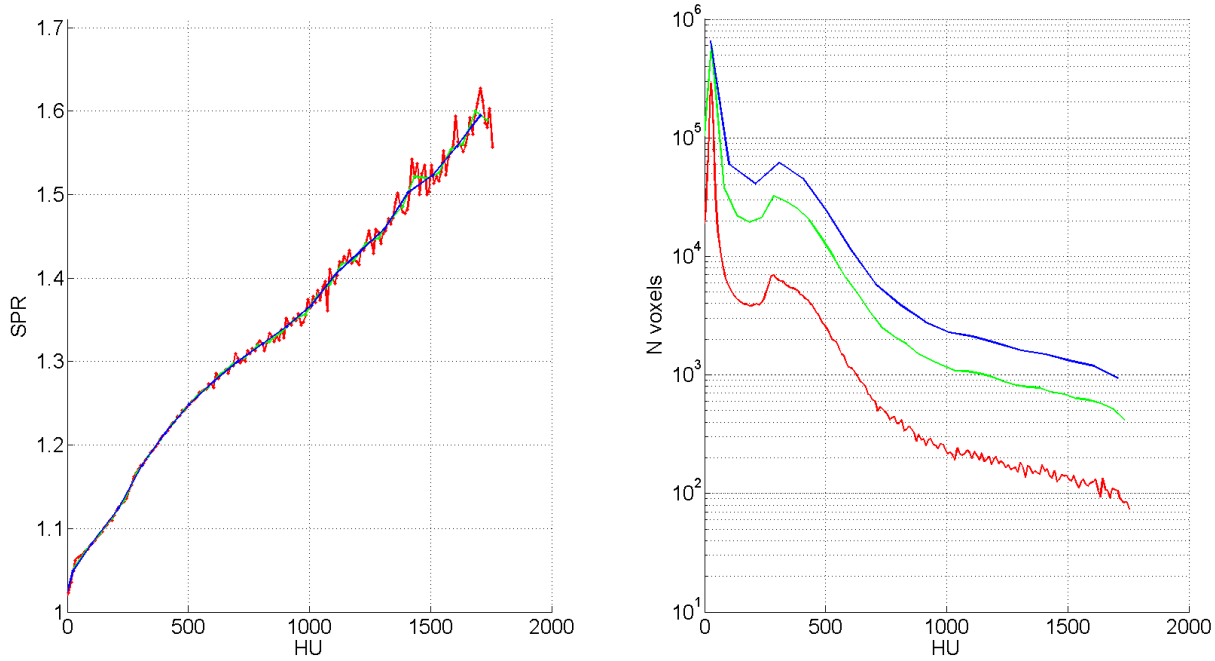

Figure 3. At the left, the calibration curves obtained by a bin size of 10HU (red line), 50HU (green) and 100HU (blue) are shown. At the right the corresponding number of averaged voxels is reported.

The cross-calibration was also compared with the standard CT calibration at TPS. The dose comparison is shown in **Figure 4** for a lateral beam and for an anterior-oblique beam optimized on the SPR map arising from pCT images, then recalculated on the SPR map arising from X-ray CT images by conventional CT calibration and by CT cross-calibration. On both the lateral beam and the anterior-oblique beam, compared to the results obtained with the pCT-based SPR map, the dose profile along a line crossing the isocenter showed a slight shift of around 1 mm at a depth of 100 mm (i.e. the range uncertainty was around 1%) of the dose fall-off on the SPR map obtained by the conventional CT calibration and almost no shift with the cross-calibration (**Figure 4D, L**). On the oblique beam, the range of the dose fall-off on the conventionally calibrated CT was around 1% longer than on pCT, while on the cross-calibrated CT it was less than 1% shorter (**Figure 4H**). With the conventional calibration, on both the lateral beam and the anterior-oblique beam, dose difference maps evidenced a range shift on the distal side (**Figure 4E,M**). Correspondingly, a marked reduction in the difference was observed by using the cross calibration (**Figure 4F,N**).

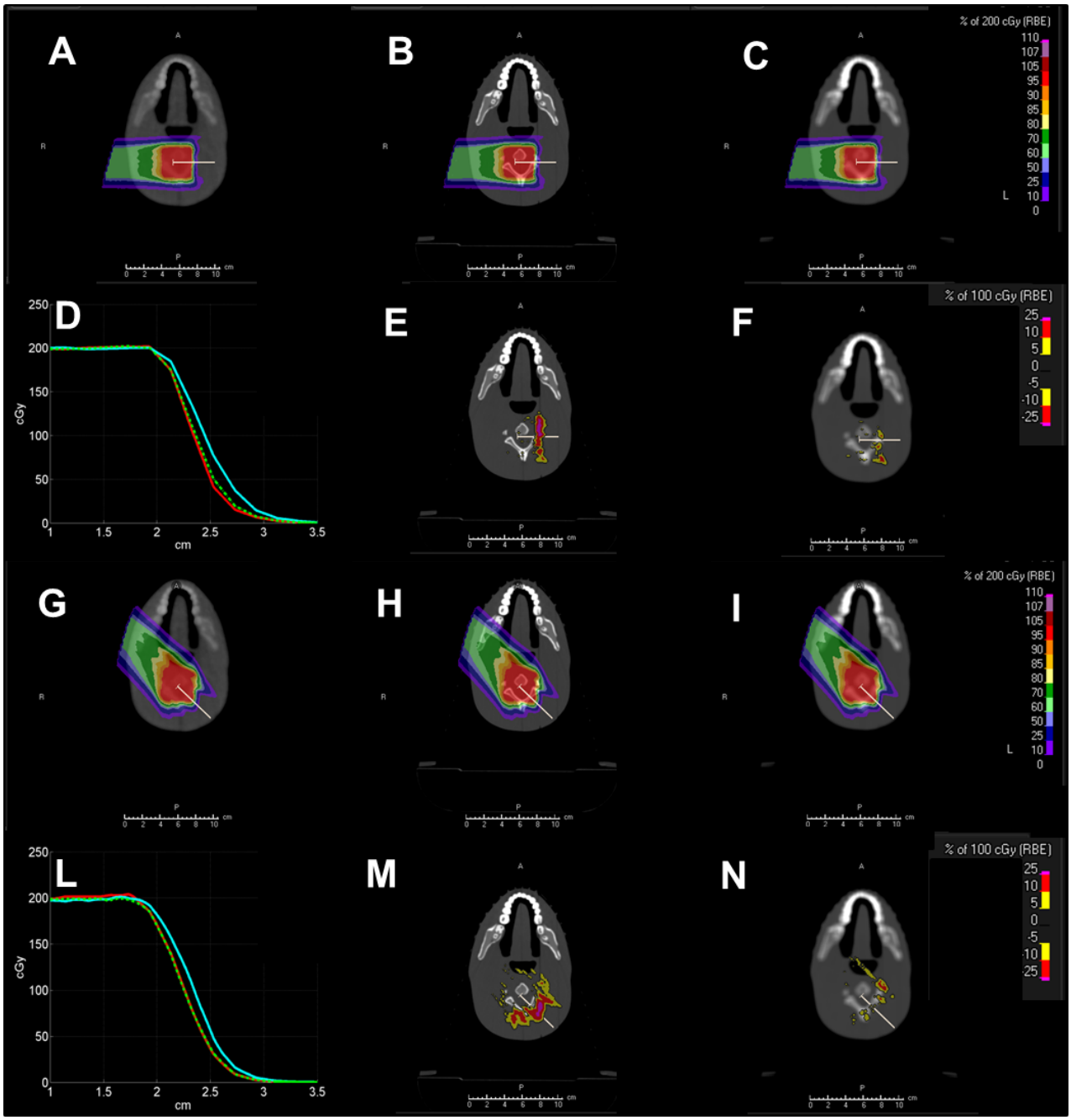

Figure 4. The dose distribution obtained with a single lateral (**A-F**) and a single oblique anterior (**G-N**) beam optimized on the SPR map arising from pCT (**A, G**) was recomputed on the SPR maps obtained by conventional x-ray CT calibration (**B, H**) and by cross-calibration (**C, I**). The corresponding dose profile along the white line in (**A-C**) and (**G-I**) are shown in (**D, L**), where the red continuous line corresponds to the dose (**A, G**), the cyan continuous line to (**B-H**) and the dashed green line to (**C, I**). Dose difference maps between **A** and **B** is shown in **E**, between **A** and **C** in **F**, between **G** and **H** in **M** and between **G** and **I** in **N**.

DISCUSSION

In this note we present the proof of concept of an innovative approach to perform x-rays CT calibration by means of a cross calibration with pCT data. The reported validation and consistency tests demonstrated that by cross-calibration with pCT an heterogeneous sample can be used, without needing homogeneous TEMs. In the reported tests, the resulting range uncertainty was around 1% or lower and therefore smaller than the range uncertainty typically adopted in robust proton treatment planning (around 3-3.5%).

It is worth noting that the conventional CT calibration was obtained by using exactly the same material that composes the phantom, thus providing an accurate calibration. This condition cannot be replicated with a real patient, as uniform samples of the corresponding tissue are not available.

Indeed, the main advantage of the cross-calibration method lies in the possibility to use a heterogeneous phantom for CT calibration instead of a phantom made of uniform samples, as required by conventional CT calibration. Uniform samples can be obtained with synthetic TEMs, but unfortunately they have limitations in mimicking the radiological properties of real biological tissues. Besides that, a heuristic function must then be applied to compute the SPR at the end of the two-step procedure to translate HU into SPR.

A calibration of the x-CT system directly using animal tissues of known SPR would produce the most reliable calibration curves. Since biological tissues are intrinsically heterogeneous, a uniform biological sample might be obtained only by homogenizing tissue samples, which would mix all the different components, thus modifying the tissue structure and properties. On the contrary, by pCT cross-calibration an actual tissue portion, even though markedly heterogeneous, could be used for the calibration procedure.

In this perspective, the main issue in the calibration chain would be the availability of a biological phantom. The production of stable phantoms is crucial in this respect. In a research project funded by the Istituto Nazionale di Fisica Nucleare (INFN), a set of dedicated biological phantoms will be designed and prepared. Once a customized and stable biological phantom will be available, this calibration procedure could be easily extended to other PT centres not equipped with a pCT system. This could be done by shipping the stable biological phantom to the remote centre for an acquisition with the x-CT systems to be calibrated, while having the corresponding SPR maps already reconstructed from pCT. The SPR map and the x-ray CT HU will be then processed and a calibration function for the remote x-CT system can be extracted. A possible flowchart is summarized in supplementary **Figure S1**, assuming a unique service provider (of the biological

phantom plus pCT data and cross-calibration software) supporting the calibration of a x-ray CT of a generic remote PT centre.

The proposed method is based on an accurate image registration followed by the association between measured SPR and HU. The method was refined by artificially blurring the x-ray CT image to degrade the spatial resolution to a level comparable to the proton CT and only then extracting the voxel-wise value pairs for further processing. A more sophisticated approach would be to explicitly formulate the image formation process in both modalities and, based on that, to devise a cost function, which compares the two images, to be minimized. Similar approaches have been used in the literature when combining x-ray CT and proton radiography. Alternatively, voxel based method by the concept of machine learning could be developed, in which part of the data is used to train (optimize) a model which is then applied on the remaining HU data to predict the SPR values. Those methods are under investigation for conversion of magnetic resonance imaging data to HU maps relevant for radiotherapy planning,[17,18] i.e. to generate the so called synthetic-CT (or pseudo-CT or similar).

Finally, it is worth noting that there are uncertainties in the x-ray image itself that are not related to the calibration. These uncertainties may originate from imperfections in the x-ray CT acquisition and reconstruction including e.g. beam hardening artefacts. In fact, these latter cause HU values of the same material to vary as a function of position within the image. Since the proposed method relies on a lookup table (as current clinical methods do), it is intrinsically unable to correct for spatially dependent uncertainties in the image. However, beam hardening and correction of imperfection in CT images is an intense field of research and it is reasonable to expect that CT image quality will be further improved in the future.

CONCLUSIONS

The data presented can be considered as a proof-of-principle of a new methodological approach for CT calibration that, based on pCT data, allows using heterogeneous phantom for CT calibration. This method overcomes the drawback of conventional CT calibration requiring homogeneous samples, which can be only obtained by synthetic TEMs. These TEMs are associated to limitations in the accurate mimicking the properties of biological tissues. The proposed method paves the way to the use of heterogeneous biological tissues for CT calibration, obtaining a more accurate description of patients' tissues by means of improved SPRs values. As a direct consequence of the reduced uncertainty, this might eventually translate into the possibility of delivering more conformal PT treatments. The same procedure could be easily adopted by other PT centers, even when not equipped with a pCT system.

DISCLOSURE OF CONFLICTS OF INTEREST

Authors have no conflict of interest to declare.

Supplementary Figure S1

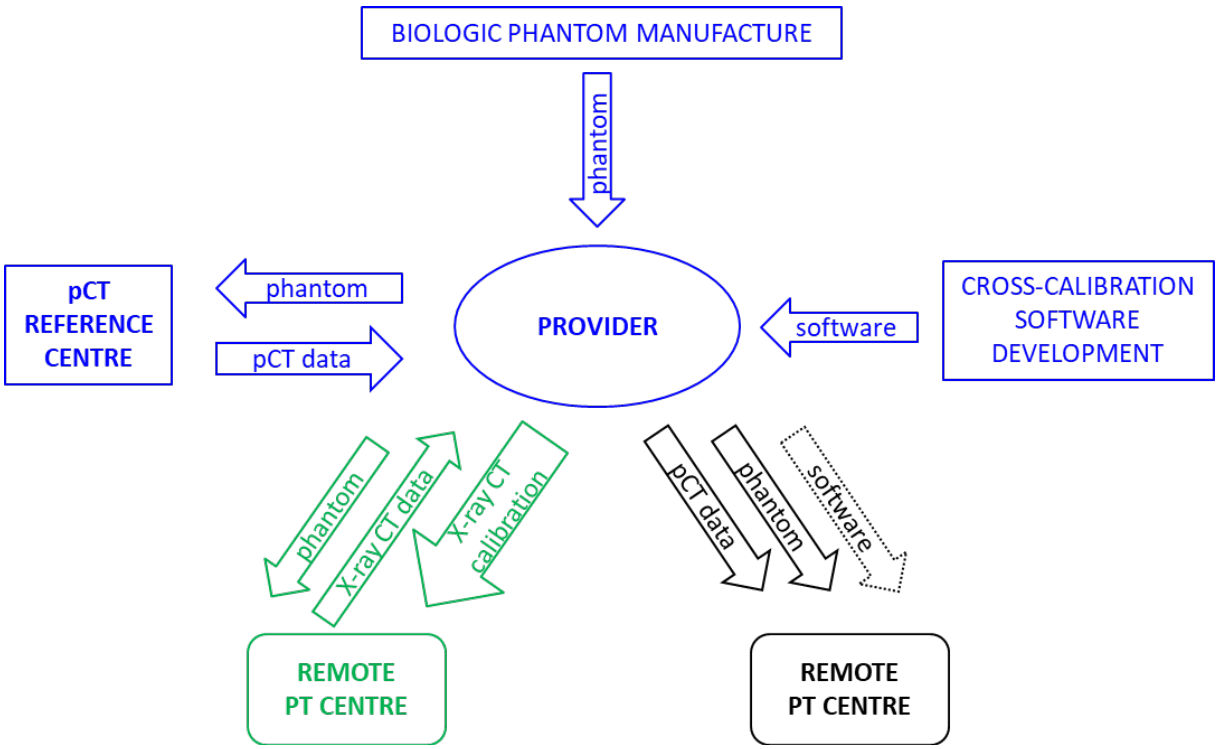

Figure 4. A possible flowchart with a unique service provider facing a generic remote proton therapy (PT) centre. The provider (blue blocks) might outsource biologic phantom manufacture, development of the cross-calibration software and pCT acquisition of the phantom. When facing with the remote centre, the provider might ship both the phantom and the corresponding pCT data (black blocks) with or without (if the remote centre prefers to develop his own procedure) the cross-calibration software (dotted line). Alternatively (green blocks), the provider might ship only the phantom, the remote centre might acquire the x-ray CT data and send them to the provider who might finally transmit the computed CT calibration.

293 **REFERENCES**

1. Yang M, Zhu XR, Park PC, Titt U, Mohan R, Virshup G, Clayton JE, Dong L. Comprehensive analysis of proton range uncertainties related to patient stopping-power-ratio estimation using the stoichiometric calibration. Phys Med Biol. 2012 Jul 7;57(13):4095-115.
2. Wohlfahrt P, Möhler C, Enghardt W, Krause M, Kunath D, Menkel S, Troost EGC, Greilich S, Richter C. Refinement of the Hounsfield look-up table by retrospective application of patient-specific direct proton stopping-power prediction from dual-energy CT. Med Phys. 2020 Apr;47(4):1796-1806.
3. Simard M, Bär E, Blais D, Bouchard H. Electron density and effective atomic number estimation in a maximum a posteriori framework for dual-energy computed tomography. Med Phys. 2020 Jun 3. doi: 10.1002/mp.14309.
4. De Smet V, Labarbe R, Vander Stappen F, Macq B, Sterpin E. Reassessment of stopping power ratio uncertainties caused by mean excitation energies using a water-based formalism. Med Phys. 2018 Jul;45(7):3361-3370.
5. Bär E, Lalonde A, Zhang R, Jee KW, Yang K, Sharp G, Liu B, Royle G, Bouchard H, Lu HM. Experimental validation of two dual-energy CT methods for proton therapy using heterogeneous tissue samples. Med Phys. 2018 Jan;45(1):48-59.
6. Farace P. Experimental verification of ion stopping power prediction from dual energy CT data in tissue surrogates. Phys Med Biol. 2014 Nov 21;59(22):7081-4.
7. Schneider U, Pemler P, Besserer J, Pedroni E, Lomax A, Kaser-Hotz B. Patient specific optimization of the relation between CT-hounsfield units and proton stopping power with proton radiography. Med Phys. 2005 Jan;32(1):195-9.
8. Meijers A, Free J, Wagenaar D, Deffet S, Knopf AC, Langendijk JA, Both S. Validation of the proton range accuracy and optimization of CT calibration curves utilizing range probing. Phys Med Biol. 2020 Feb 4;65(3):03NT02.
9. Doolan PJ, Testa M, Sharp G, Bentefour EH, Royle G, Lu HM. Patient-specific stopping power calibration for proton therapy planning based on single-detector proton radiography. Phys Med Biol. 2015 Mar 7;60(5):1901-17.
10. Collins-Fekete CA, Brousmiche S, Hansen DC, Beaulieu L, Seco J. Pre-treatment patient-specific stopping power by combining list-mode proton radiography and x-ray CT. Phys Med Biol. 2017 Aug 3;62(17):6836-6852.

11. Krah N, Patera V, Rit S, Schiavi A, Rinaldi I. Regularised patient-specific stopping power calibration for proton therapy planning based on proton radiographic images. Phys Med Biol. 2019 Mar 12;64(6):065008.
12. Zhang R, Sharp GC, Jee KW, Cascio E, Harms J, Flanz JB, Lu HM. Iterative optimization of relative stopping power by single detector based multi-projection proton radiography. Phys Med Biol. 2019 Mar 18;64(6):065022.
13. Dedes G, Dickmann J, Niepel K, Wesp P, Johnson RP, Pankuch M, Bashkirov V, Rit S, Volz L, Schulte RW, Landry G, Parodi K. Experimental comparison of proton CT and dual energy x-ray CT for relative stopping power estimation in proton therapy. Phys Med Biol. 2019 Aug 14;64(16):165002.
14. C. Civinini et al. Relative Stopping Power Measurements and Prosthesis artifacts reduction in proton CT. Phys. Med. Biol. 2020 (in press) https://doi.org/10.1088/1361-6560/abb0c8
15. Tommasino F, Widesott L, Fracchiolla F, Lorentini S, Righetto R, Algranati C, Scifoni E, Dionisi F, Scartoni D, Amelio D, Cianchetti M, Schwarz M, Amichetti M, Farace P. Clinical implementation in proton therapy of multi-field optimization by a hybrid method combining conventional PTV with robust optimization. Phys Med Biol. 2020 Feb 10;65(4):045002.
16. Kanematsu N, Inaniwa T, Nakao M. Modeling of body tissues for Monte Carlo simulation of radiotherapy treatments planned with conventional x-ray CT systems. Phys Med Biol. 2016 Jul 7;61(13):5037-50.
17. Johansson A, Karlsson M, Nyholm T. CT substitute derived from MRI sequences with ultrashort echo time. Med Phys. 2011 May;38(5):2708-14.
18. Johansson A, Karlsson M, Yu J, Asklund T, Nyholm T. Voxel-wise uncertainty in CT substitute derived from MRI. Med Phys. 2012 Jun;39(6):3283-90.